J. Fluid Mech. (1979), *vol.* 94, *part* 3, *pp.* 497–517
Printed in Great Britain

The trajectories of particles in steep, symmetric gravity waves

By M. S. LONGUET-HIGGINS

Department of Applied Mathematics and Theoretical Physics,
Silver Street, Cambridge, and Institute of Oceanographic Sciences, Wormley, Surrey

(Received 19 October 1978)

To gain insight into the orbital motion in waves on the point of breaking, we first study the trajectories of particles in some ideal irrotational flows, including Stokes' 120° corner-flow, the motion in an almost-highest wave, in periodic deep-water waves of maximum height, and in steep, solitary waves.

In Stokes' corner-flow the particles move as though under the action of a constant force directed away from the crest. The orbits are expressible in terms of an elliptic integral. The trajectory has a loop or not according as $q \lessgtr c$ where q is the particle speed at the summit of each trajectory, in a reference frame moving with speed c. When $q = c$, the trajectory has a cusp. For particles near the free surface there is a sharp vertical gradient of the horizontal displacement.

The trajectories of particles in almost-highest waves are generally similar to those in the Stokes corner-flow, except that the sharp drift gradient at the free surface is now absent.

In deep-water irrotational waves of maximum steepness, it is shown that the surface particles advance at a mean speed U equal to $0{\cdot}274c$, where c is the phase-speed. In solitary waves of maximum amplitude, a particle at the surface advances a total distance 4·23 times the depth h during the passage of each wave. The initial angle α which the trajectory makes with the horizontal is close to 60°.

The orbits of subsurface particles are calculated using the 'hexagon' approximation for deep-water waves. Near the free surface the drift has the appearance of a thin forwards jet, arising mainly from the flow near the wave crest. The vertical gradient is so sharp, however, that at a mean depth of only $0{\cdot}01L$ below the surface (where L is the wavelength) the forwards drift is reduced to less than half its surface value. Under the action of viscosity and turbulence, this sharp gradient will be modified. Nevertheless the orbital motion may contribute appreciably to the observed 'wind-drift current'.

Implications for the drift motions of buoys and other floating bodies are also discussed.

1. Introduction

In progressive gravity waves of very small amplitude it is well known that the orbits of the particles are either elliptical or circular (see Lamb 1932, ch. 9). In steep waves, however, the orbits become quite distorted, as is shown by the existence of a mean horizontal drift or mass-transport in irrotational waves (Stokes 1847; Rayleigh

0022-1120/79/4284–7090 $02.00

1876). In the extreme case of very steep waves the calculation of the trajectories has dresented some difficulty owing to the unavailability, till recently, of suitable approximations for steep waves. To some extent this difficulty has been overcome in recent papers by the present author (1973, 1974, 1979) and the main purpose of the present paper is to take advantage of these approximations to determine the qualitative and quantitative behaviour of the particle orbits in steep waves.

A second and more general obstacle has been to find an appropriate transformation from the description of a wave motion in Eulerian co-ordinates, which are most suitable for steady, irrotational motions, to a more Lagrangian type of description. (It will be recalled that Gerstner's exact solution in Lagrangian co-ordinates, being highly rotational, has correspondingly little physical interest.) Even the exact Eulerian solution represented by Stokes' simple corner-flow (1880) appears not to have been considered from a Lagrangian viewpoint, in spite of its obvious interest and relevance to steep gravity waves.

In § 2 of the present paper we therefore determine analytically the trajectories in Stokes' corner-flow. It turns out that each fluid particle moves as though it were under the action of a central force of constant strength, directed away from the crest of the wave. The resulting trajectory is described analytically by known functions, in the form of an elliptic integral. Paradoxically, the orbit of a particle at the surface is smooth even at the highest point, precisely where the free surface has a discontinuity in slope.

In § 4 we consider the particle trajectories near the crest of a steep but still rounded wave, and here we make use of a simple but accurate approximation to the flow in the crest found very recently (Longuet-Higgins 1979). Again the solutions are expressible in terms of known functions, so that we have an addition (though admittedly only an approximate one) to the limited number of known solutions in Lagrangian variables.

The results of §§ 2 and 4 apply in practice only to the upper part of progressive waves. To determine the complete trajectory of surface particles in a periodic wave, we use in § 5 the form of the wave of maximum amplitude as calculated by Yamada (1957). We find, for example, that in each complete orbit a particle advances horizontally through a distance 0·38 times the wavelength, and that its mean speed of advance is 0·27 times the phase speed.

In § 6 we consider the solitary wave of maximum amplitude, and find the trajectory of a particle at the surface during the passage of each wave. Subsurface trajectories for periodic waves are studied in § 7. Here the hexagon approximation for deep-water waves (Longuet-Higgins 1973) is found particularly useful. The calculations reveal the presence of a sharp gradient in the drift near the free surface, when viscous forces are neglected.

In § 8 we discuss the applicability of these results to real waves, both in laboratory channels and in the ocean.

2. The Stokes corner-flow

Suppose the crest travels to the right, and first let us take axes attached to the crest as in figure 1, with the y axis horizontal and the x axis vertically downwards. We write

$$z = x + iy = re^{i\theta}. \tag{2.1}$$

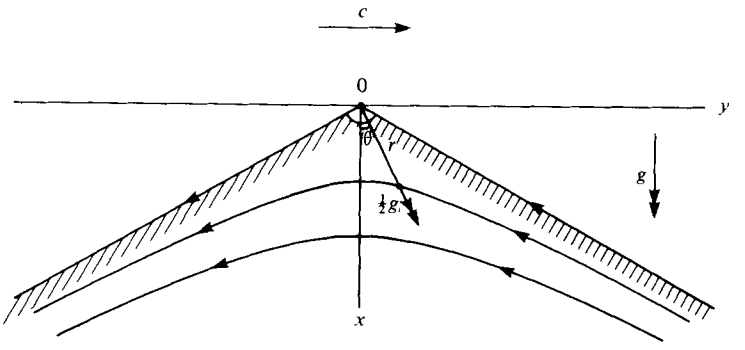

FIGURE 1. Co-ordinates for the Stokes' corner-flow, and streamlines of the motion relative to moving axes.

Then if
$$\chi = \phi + i\psi \tag{2.2}$$
denotes the complex velocity potential, the components of velocity u, v in the x, y directions are given by
$$w = u + iv = (d\chi/dz)^* \tag{2.3}$$
a star denoting the complex conjugate.

Stokes' solution (1880) for the corner-flow, in Eulerian co-ordinates, can be written
$$\chi = iCz^{\frac{3}{2}}, \quad -\tfrac{1}{3}\pi \leqslant \theta \leqslant \tfrac{1}{3}\pi, \tag{2.4}$$
where
$$C = \tfrac{2}{3}g^{\frac{1}{2}} \tag{2.5}$$
and g denotes the acceleration due to gravity. From (2.3) this implies the simple relation
$$w = u + iv = -i(gz^*)^{\frac{1}{2}} \tag{2.6}$$
for the velocity. This is of course steady and independent of the time t, in the relative frame of reference.

Now to find the trajectory of a given particle, let Z be the position of a particle referred to Lagrangian co-ordinates. From (2.6) we have then
$$dZ/dt = w = -i(gZ^*)^{\frac{1}{2}}, \tag{2.7}$$
so
$$\frac{d^2Z}{dt^2} = -\tfrac{1}{2}i\left(\frac{g}{Z^*}\right)^{\frac{1}{2}}\frac{dZ^*}{dt} = \tfrac{1}{2}g\left(\frac{Z}{Z^*}\right)^{\frac{1}{2}}. \tag{2.8}$$
Since
$$(Z/Z^*)^{\frac{1}{2}} = e^{i\theta} \tag{2.9}$$
it follows that the particle acceleration is everywhere equal to $\frac{1}{2}g$ directed away from the crest (as shown differently by Longuet-Higgins 1963). Hence each fluid particle moves exactly as if it were in a central field of force, of constant strength, with centre of repulsion at the crest.

Now for a particle in any central field of force the angular momentum about the origin is invariant (see for example Ramsey 1937). This result is equivalent to Kepler's second law, that the area swept out by the radius vector from the sun to a planet increases uniformly with the time. Hence we have
$$r^2 d\theta/dt = \text{constant} = A \tag{2.10}$$

say. The value of A can be found from the fact that $r\,d\theta/dt = r^{-1}\partial\phi/\partial\theta$, so

$$A = \partial\phi/\partial\theta = -g^{\frac{1}{2}}r^{\frac{1}{2}}\cos\tfrac{1}{2}\theta = -g^{\frac{1}{2}}h^{\frac{1}{2}}, \tag{2.11}$$

where h denotes the height of the origin above the trajectory at its mid-point $\theta = 0$. It is easily seen also that $A = -\frac{3}{2}\psi$. Now from (2.11) we have

$$r^2\cos^{\frac{4}{3}}(\tfrac{3}{2}\theta) = h^2 \tag{2.12}$$

and so from (2.10) and (2.12), provided $h \neq 0$, we obtain

$$\frac{d\theta}{dt}\sec^{\frac{4}{3}}(\tfrac{3}{2}\theta) = A/h^2 = -(g/h)^{\frac{1}{2}}. \tag{2.13}$$

Hence

$$t = -\left(\frac{h}{g}\right)^{\frac{1}{2}}\int_0^\theta \sec^{\frac{4}{3}}(\tfrac{3}{2}\theta)\,d\theta. \tag{2.14}$$

Lastly setting

$$\tan(\tfrac{3}{2}\theta) = -\mu \tag{2.15}$$

we obtain

$$t = \frac{2}{3}\left(\frac{h}{g}\right)^{\frac{1}{2}}\int_0^\mu \frac{d\mu}{(1+\mu^2)^{\frac{1}{3}}}. \tag{2.16}$$

The integral on the right is an elliptic integral, expressible in terms of known functions (see Bowman 1953). In practice, however, it can be evaluated readily by numerical quadrature, using Simpson's rule or other convenient methods.

In a progressive motion, where the wave crest travels to the right with speed c, the trajectory of a particle will be given by co-ordinates $X = x$, $Y = y + ct$ where from (2.4)

$$x + iy = (\chi/iC)^{\frac{2}{3}} = C^{-\frac{2}{3}}(\psi - i\phi)^{\frac{2}{3}} = h(1-i\mu)^{\frac{2}{3}} \tag{2.17}$$

and t is given by (2.16). As in (2.16) we have written $\mu = \phi/\psi = -\tan(\frac{3}{2}\theta)$. It is convenient to define a natural length-scale

$$l = c^2/g \tag{2.18}$$

(so that the length of a deep-water wave is roughly $2\pi l$) and a dimensionless parameter for each trajectory, namely

$$\kappa \equiv h/l = gh/c^2 = q^2/c^2, \tag{2.19}$$

where q is the particle speed at the summit of the trajectory, in the steady motion. Then from (2.16) and (2.17) we find

$$\frac{X+iY}{l} = \kappa(1-i\mu)^{\frac{2}{3}} + \tfrac{2}{3}i\kappa^{\frac{1}{2}}\int_0^\mu \frac{d\mu}{(1+\mu^2)^{\frac{1}{3}}} \tag{2.20}$$

(see figures 2 and 3).

The case $\kappa = 0$, when the particle is on the free surface, requires separate consideration, but this is very simple. For, a particle at the free surface (say on the forward face) behaves as though it were on a smooth plane inclined at an angle $-30°$ to the horizontal. Hence

$$\frac{d^2X}{dt^2} = \tfrac{1}{4}g, \quad \frac{d^2Y}{dt^2} = \frac{3^{\frac{1}{2}}}{4}g. \tag{2.21}$$

Since the velocity at the crest is horizontal and equal to c we have by integration simply

$$X/l = \tfrac{1}{8}\tau^2, \quad Y/l = \tau + \frac{3^{\frac{1}{2}}}{8}\tau^2, \tag{2.22}$$

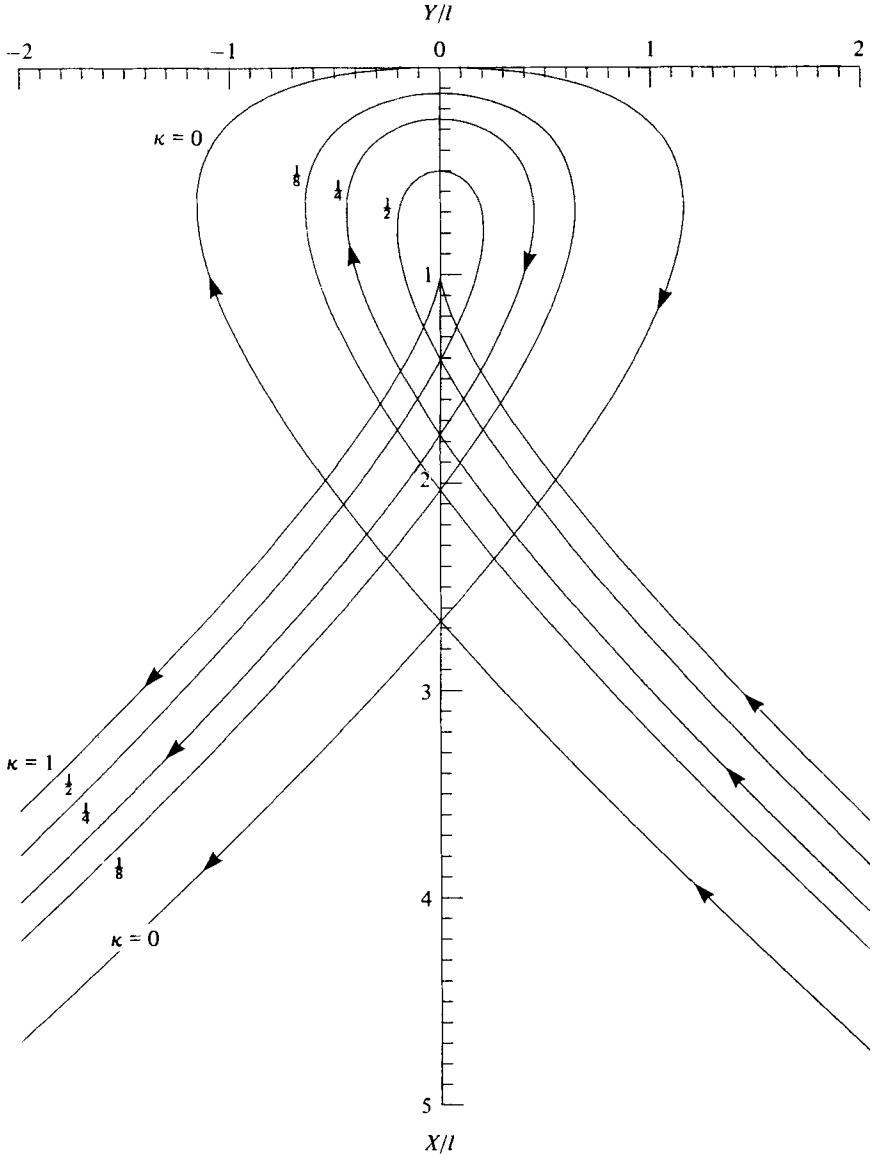

FIGURE 2. Trajectories of particles in the Stokes' corner flow, relative to fixed axes: $\kappa = 0, \frac{1}{8}, \frac{1}{4}, \frac{1}{2}$ and 1.

where $\tau = gt/c$. At the crest itself there is a discontinuity in the acceleration, but no discontinuity in the velocity, and the orbit is therefore apparently smooth. On the two sides of the origin the trajectories take the forms of parabolas with axes inclined at angles $\pm 30°$ to the vertical and passing through the point $Y = 0$, $X = l$. The parabolas intersect in the plane of the symmetry at a distance $X = \frac{8}{3}l$ below the crest.

In figure 2 we have plotted the trajectories for $\kappa = 0, \frac{1}{8}, \frac{1}{4}, \frac{1}{2}$ and 1. The motion is in each case forwards at the crest, except that when $\kappa = 1$ the trajectory has a cusp at

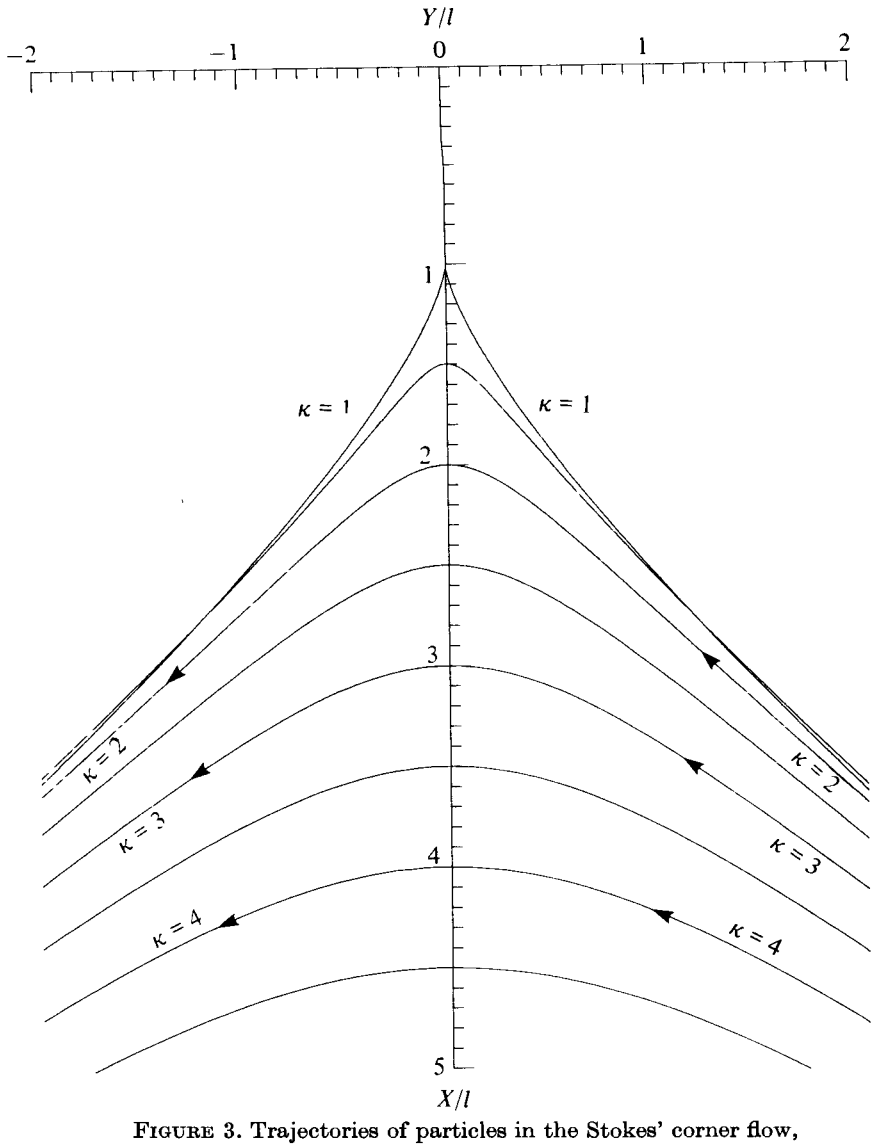

FIGURE 3. Trajectories of particles in the Stokes' corner flow, relative to fixed axes: $\kappa = 1, 1{\cdot}5, 2{\cdot}0, \ldots, 4{\cdot}5$.

$X = l$. In figure 3 are plotted the trajectories for $\kappa = 1{\cdot}0\ (0{\cdot}5)\ 4{\cdot}5$ showing that when $\kappa > 1$ the flow is always backwards.

In applying the result to periodic waves, it must be borne in mind that the corner-flow applies only to a region near the crest, of diameter small compared to the wavelength. Hence for waves in deep water, for example, we should have X and Y both small compared to l. The complete particle orbits for progressive waves will be investigated in §§ 5 and 6.

3. Time-integration in steady flows: a general method

The following is a general method for determining the trajectories of particles in a progressive wave (reducible to a steady flow) when the Eulerian co-ordinate z is given as a function of χ, instead of vice versa.

Let D/Dt denote differentiation following a particle. Then since $Dz/Dt = w = (d\chi/dz)^*$ we have in a steady flow

$$\frac{D\chi}{Dt} = \frac{d\chi}{dz}\frac{Dz}{Dt} = \frac{d\chi}{dz}\left(\frac{d\chi}{dz}\right)^*. \tag{3.1}$$

Taking real and imaginary parts of each side we get

$$\left.\begin{aligned} \frac{D\phi}{Dt} &= \frac{d\chi}{dz}\left(\frac{d\chi}{dz}\right)^*, \\ \frac{D\psi}{Dt} &= 0. \end{aligned}\right\} \tag{3.2}$$

The second of these equations tells us only that ψ is constant on a streamline, but from the first we have on integration

$$t = \int \frac{dz}{d\chi}\left(\frac{dz}{d\chi}\right)^* d\phi. \tag{3.3}$$

Since ψ is constant in the integrand, this gives us t as a function of ϕ or χ, and vice versa. From $z(\chi)$ we then find z as a function of t. To convert to a stationary frame of reference we simply add to the horizontal co-ordinate the term ct.

The expression (3.3) is equivalent to the formula $t = \int d\phi/q^2$ used by Rayleigh (1876) and others in discussing the mass-transport velocities in an irrotational wave.

Clearly this method can be applied to the Stokes corner-flow in § 2. Thus starting from (2.4) we have $z = (\chi/iC)^{\frac{2}{3}}$ and hence

$$t = \left(\frac{2}{3g}\right)^{\frac{2}{3}} \int \frac{d\phi}{(\chi\chi^*)^{\frac{1}{3}}} = \left(\frac{2}{3g}\right)^{\frac{2}{3}} \int \frac{d\phi}{(\phi^2+\psi^2)^{\frac{1}{3}}}, \tag{3.4}$$

which is equivalent to (2.16) when we write $\mu = \phi/\psi$. This approach, however, misses the physical interpretations given above.

In §§ 4 and 8 the general formula (3.3) will be applied to determine the particle orbits in some other interesting cases.

4. Trajectories in the almost-highest wave

In steep waves, short of the highest, the free surface is still rounded at the crest. When the radius of curvature is not zero but is still small compared to the wavelength or the depth, it can be shown that the flow near the crest approaches asymptotically a limiting form, whose scale is determined simply by the radius of curvature at the summit. The precise form of this asymptotic flow has been calculated by Longuet-Higgins & Fox (1977).

For our purpose it will be convenient to use a simple but very close approximation derived in a companion paper (Longuet-Higgins 1979). If we take $g = 1$ and the unit of length as $q^2/2g$, where q denotes the particle speed at the crest in a reference frame

moving to the right with the phase speed then it was shown that the expression for z as function of χ is simply

$$z = \frac{\alpha - \gamma i\chi}{(\beta - i\chi)^{\frac{1}{3}}}, \tag{4.1}$$

where α, β and γ are constants:

$$\left.\begin{aligned} \beta &= \frac{2^{\frac{8}{3}}}{3^{\frac{1}{2}} - 15} = 4{\cdot}8065, \\ \alpha &= \beta^{\frac{1}{3}} = 1{\cdot}6876, \\ \gamma &= (\tfrac{3}{2})^{\frac{2}{3}} = 1{\cdot}3104. \end{aligned}\right\} \tag{4.2}$$

The free surface at its highest point passes through the point $z = 1$ where $q^2 = 2$ precisely. And at infinity we have

$$z \sim (-\tfrac{3}{2}i\chi)^{\frac{2}{3}} \tag{4.3}$$

in agreement with equation (2.4).

To find the particle trajectories we have first from (4.1)

$$\frac{dz}{id\chi} = \frac{\delta + \epsilon i\chi,}{(\beta - i\chi)^{\frac{4}{3}}}, \tag{4.4}$$

where

$$\delta = \tfrac{1}{3}\alpha - \beta\gamma = -2^{-\frac{1}{2}}\beta^{\frac{4}{3}}; \quad \epsilon = \tfrac{2}{3}\gamma. \tag{4.5}$$

So from the general formula (3.3) we obtain

$$t = \int \frac{\zeta^2 + \epsilon^2\phi^2}{(\eta^2 + \phi^2)^{\frac{4}{3}}} d\phi, \tag{4.6}$$

where we have written

$$\zeta = \delta - \epsilon\psi, \quad \text{and} \quad \eta = \beta + \psi, \tag{4.7}$$

which are constants during the integration. The integral (4.6) is an elliptic integral, expressible, as before, in terms of known functions.

In a stationary reference frame the trajectories are given by

$$X + iY = z + ict. \tag{4.8}$$

Introducing as before the length $l = c^2/g$, we have from (4.1) and (4.6)

$$\frac{X + iY}{l} = \frac{1}{c^2}\frac{\alpha - \gamma i\chi}{(\beta - i\chi)^{\frac{1}{3}}} + \frac{i}{c}\int \frac{\zeta^2 + \epsilon^2\phi^2}{(\eta^2 + \phi^2)^{\frac{4}{3}}} d\phi. \tag{4.9}$$

The vertical distance H of the highest point of the trajectory below the origin is given by

$$\frac{H}{l} = \frac{1}{c^2}\frac{\alpha + \gamma\psi}{(\beta + \psi)^{\frac{1}{3}}}. \tag{4.10}$$

The relative speed q of a particle at the highest point ($\phi = 0$) is given by

$$\frac{q^2}{c^2} = \frac{\eta^{\frac{8}{3}}}{c^2\zeta^2} = \frac{1}{c^2}\frac{(\beta + \psi)^{\frac{8}{3}}}{(\delta - \epsilon\psi)^2}. \tag{4.11}$$

In particular for a particle at the free surface ($\psi = 0$),

$$\frac{H}{l} = \frac{1}{c^2}, \quad \frac{q^2}{c^2} = \frac{2}{c^2} \tag{4.12}$$

in the units that we have chosen.

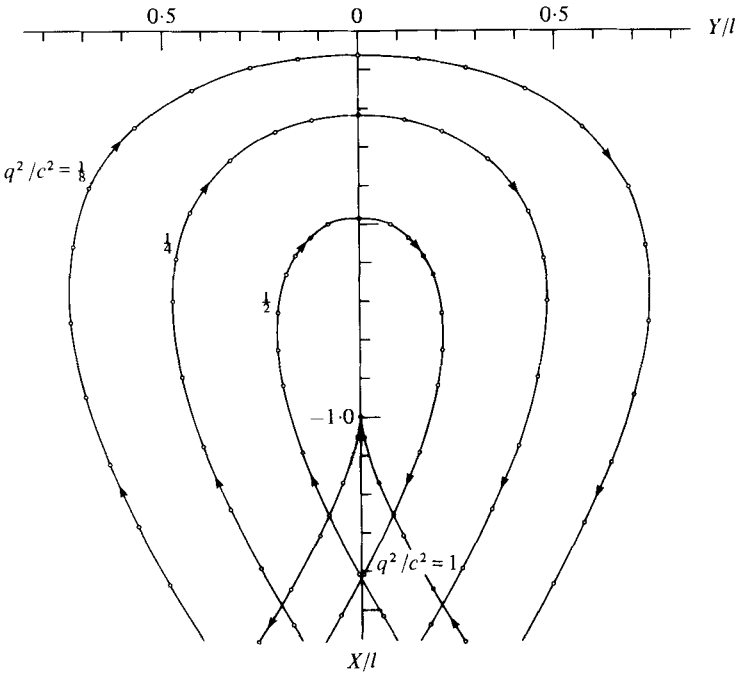

FIGURE 4. Trajectories of particles in the almost-highest wave, for $\kappa = \frac{1}{8}, \frac{1}{4}, \frac{1}{2}$ and 1, when $q^2/c^2 = \frac{1}{16}$.

c^2	q^2	ψ	H/l	q^2/c^2
16	2	0·0000	0·0625	0·125
16	4	4·2687	0·2182	0·250
16	8	14·7314	0·4871	0·500
16	16	42·7706	0·9958	1·000

TABLE 1

It is interesting to compare the particle orbits with those in figure 2 when $2/c^2$ is equal to the corresponding value of q^2/c^2 for one of the inner trajectories, say the trajectory $\kappa = 0{\cdot}125$. Then in our present units we must have $c^2 = 16$, hence

$$H/l = 0{\cdot}0625.$$

This is the uppermost trajectory in figure 4. The remaining trajectories correspond to the lower trajectories in figure 2, that is to say $\kappa = 0{\cdot}25$, 0·5 and 1·0, or $q^2 = 4$, 8 and 16 respectively. The corresponding values of ψ are found from (4.11), or rather

$$\frac{(\beta+\psi)^{\frac{3}{2}}}{\delta-\epsilon\psi} = -q, \tag{4.13}$$

where the positive value of q is taken. When $q = c = 4$ the trajectory has a cusp. This corresponds to $\psi = 42{\cdot}770$, $H/l = 0{\cdot}9958$. The corresponding values of q^2/c^2 from equation (4.10) are shown in table 1. From this it is clear that when $x/l \geqslant 0{\cdot}5$ the trajectories differ little from those in the highest wave. However, close to the

crest they are appreciably different. In particular, the almost-highest wave does not have the very sharp gradient of orbital motion that is found in the Stokes' 120° corner-flow for particles close to the free surface.

5. Periodic waves in deep water: surface particles

The particle trajectories found in §§ 2 and 4 above will apply strictly only to particles in the neighbourhood of a wave crest, that is to say to the uppermost part of the orbits in a periodic wave. To obtain the complete orbits, we shall consider first a specially simple case, that of the highest progressive wave in deep water (see figure 5).

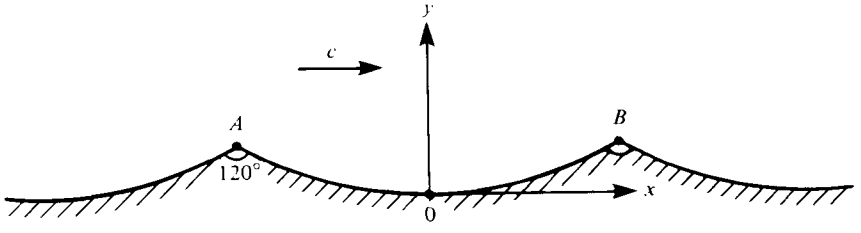

FIGURE 5. Axes and co-ordinates for the highest gravity wave in deep water.

For particles at the free surface the pressure is constant, so that we can use Bernoulli's equation. Thus if y denotes the vertical displacement of the free surface (positive upwards) as a function of the horizontal† co-ordinate x then (in a frame of reference moving with the phase-speed) we shall have for the particle speed q at any instant

$$q^2 = 2g(y_0 - y), \tag{5.1}$$

where y_0 is the value of y at the sharp crest (corresponding to $q = 0$). But if

$$\theta = \arctan(dy/dx)$$

denotes the inclination of the free surface to the horizontal we shall have

$$dx/dt = -q\cos\theta,$$

hence

$$(dx/dt)^2(1+\tan^2\theta) = 2g(y_0 - y). \tag{5.2}$$

Therefore by integration

$$t = -\frac{1}{(2g)^{\frac{1}{2}}}\int\left\{\frac{1+(dy/dx)^2}{y_0-y}\right\}^{\frac{1}{2}}dx. \tag{5.3}$$

If $y(x)$ is given, this relation serves to determine t as a function of x. To avoid the square-root singularity at $y = y_0$ it is convenient to write

$$t = \left(\frac{2}{g}\right)^{\frac{1}{2}}\int\{(\xi/\eta)^2 + (d\eta/d\xi)^2\}^{\frac{1}{2}}d\xi. \tag{5.5}$$

† For the rest of this paper we use the more usual notation; there will be no confusion with §§ 2 and 4.

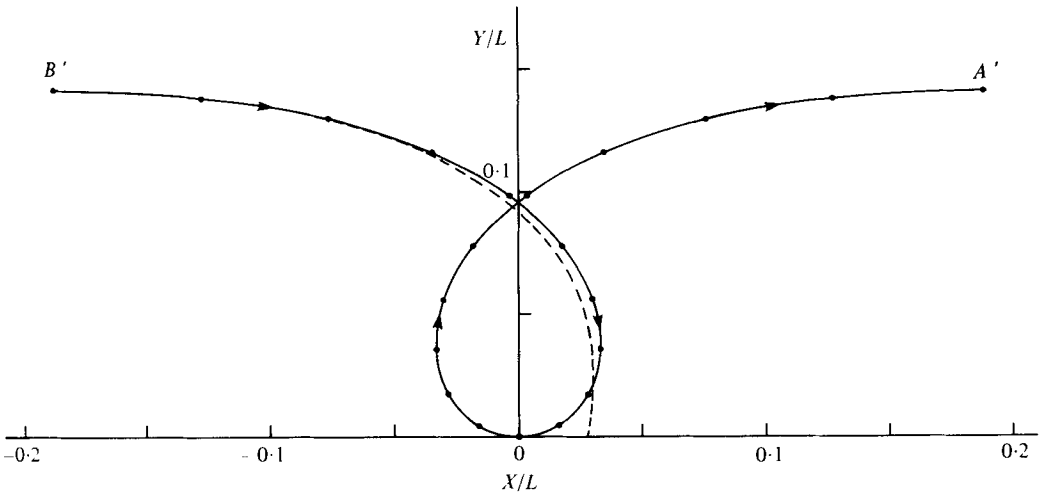

FIGURE 6. The trajectory of a surface particle in a deep-water wave of maximum height, for Yamada's profile. The broken line shows the corner-flow trajectory (5.13).

The profile of a deep-water wave of maximum height was accurately calculated by Yamada (1957) and also Schwartz (1974). Using the co-ordinates of points (x, y) on the profile as given in Yamada's table 2, we have calculated t from (5.5) and in figure 6 have plotted the particle trajectory

$$x_0 - x = \xi^2, \quad y_0 - y = \eta^2, \tag{5.4}$$

where x_0 is the x co-ordinate of the wave-crest, and then (5.3) reduces to

$$X = x + ct, \quad Y = y, \tag{5.6}$$

where c is the calculated phase speed:

$$c = 1{\cdot}0923(gL/2\pi)^{\frac{1}{2}}. \tag{5.7}$$

Further data are given in table 2 below. The total time T taken for the particle to describe a complete orbit (twice the last entry in table 2) is

$$T = 3{\cdot}1591(L/g)^{\frac{1}{2}}. \tag{5.8}$$

In this time the particle has advanced a distance $(cT - L)$, and so its mean speed of advance U is given by

$$U = (cT - L)/T = c(1 - L/cT). \tag{5.9}$$

With the above values of c and T one obtains

$$U/c = 1 - L/cT = 0{\cdot}274. \tag{5.10}$$

In other words, the mean speed of advance is a little over one-quarter of the phase velocity. The proportion of a wavelength advanced in each complete orbit is given by

$$\frac{[X]}{L} = \frac{cT - L}{L} = \frac{cT}{L} - 1 = 0{\cdot}377. \tag{5.11}$$

X/L	Y/L	$(g/L)^{\frac{1}{2}}t$	X/L	Y/L	$(g/L)^{\frac{1}{2}}t$
0·0000	0·0000	0·0000	0·0034	0·0985	0·9716
− ·0165	·0049	·1801	·0347	·1162	1·1237
− ·0282	·0175	·3483	·0758	·1298	1·2755
− ·0331	·0354	·5091	·1271	·1383	1·4275
− ·0300	·0562	·6654	·1883	·1412	1·5795
− ·0180	·0779	·8191			

TABLE 2. Co-ordinates of points on the trajectory of a particle at the surface of a deep-water wave of maximum amplitude.

From § 2, we would expect the upper part of the trajectory in figure 6 to be approximated by the two parabolas

$$\left.\begin{aligned}(X-X_0)/L &= (\tau \pm (3\tfrac{1}{2}/8)\tau^2)\,(l/L)\\ \text{and}\qquad (Y-Y_0)/L &= -\tfrac{1}{8}\tau^2(l/L),\end{aligned}\right\} \tag{5.12}$$

where $l = c^2/g$ and $\tau = (t-t_0)\,g/c$. These expressions would be exact if the free surface continued to have a downward slope of 30°, as at the crest. In fact, equations (5.12) give correctly the curvature of the trajectory at its highest point. To compare (5.12) with the exact orbit we take into account that

$$l = 1{\cdot}1932(L/2\pi) = 0{\cdot}1899L. \tag{5.13}$$

The parabolic curve is shown in figure 6 by the broken line. It will be seen that it lies remarkably close to the other curve, down as far as the lowest part of the orbit, $Y/L < 0{\cdot}03$.

6. The highest solitary wave

As an example of a wave in water of finite depth we take the extreme case of the solitary wave, where the ratio of wavelength to depth is infinite.

Taking $g = 1$ as before, and the undisturbed depth h as unity also, we may adopt for the surface profile the expression

$$y = Ae^{-\alpha|x|} + Be^{-\beta|x|}, \tag{6.1}$$

where

$$\left.\begin{aligned}A &= 1{\cdot}5389, \quad \alpha = 1{\cdot}0495,\\ B &= -0{\cdot}7093, \quad \beta = 1{\cdot}4630,\end{aligned}\right\} \tag{6.2}$$

and

$$F^2 \equiv c^2/gh = 1{\cdot}6592 \tag{6.3}$$

(see Longuet-Higgins 1974). This was shown to agree with Yamada's numerically calculated profile (Yamada 1958) within about $0{\cdot}002h$. Substituting into the general formulae (5.3) and (5.5) we can immediately find the orbital time t for a particle at the surface, and from (5.6) the co-ordinates (X, Y) of a point on the trajectory. We measure X and Y horizontally and vertically from a point at the undisturbed water level, directly below the highest point of the trajectory (see figure 7).

In figures 7 and 8 the central curve corresponds to the passage of a single solitary wave (see also table 3). The maximum height of the trajectory equals the wave height,

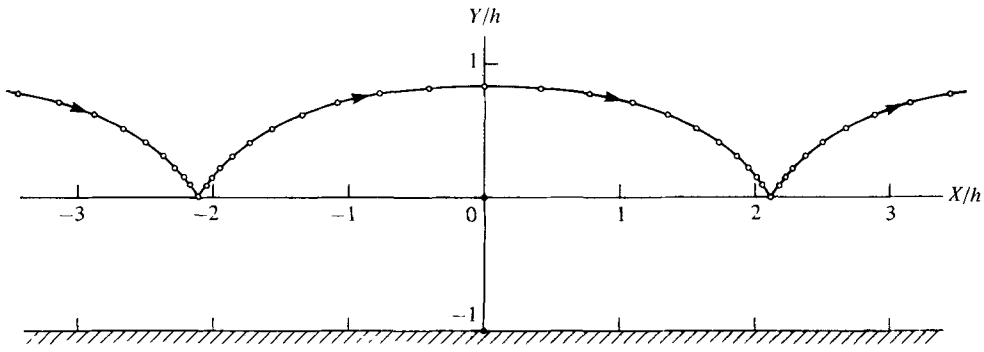

FIGURE 7. Trajectory of a surface particle in a solitary wave, with no return flow.

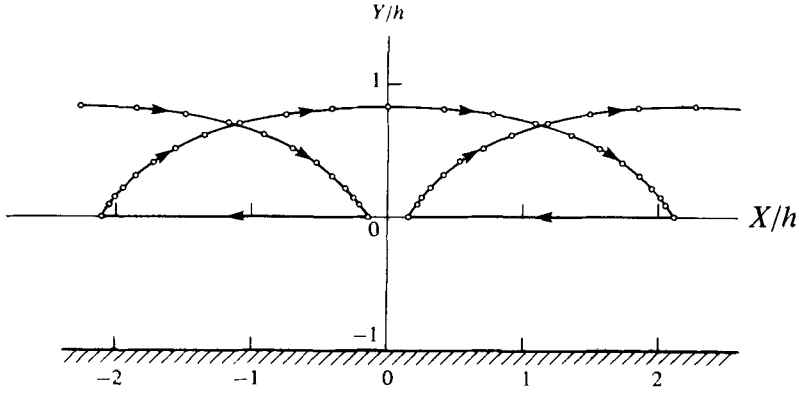

FIGURE 8. Trajectory of a surface particle in a solitary wave, with mass flux compensated by a uniform return flow.

$0{\cdot}829h$, and during each hop the particle is displaced forwards through a total distance $4{\cdot}229h$. The trajectory rises initially at an angle θ given by

$$\tan\theta \sim \frac{d^2Y}{dt^2}\Big/\frac{d^2X}{dt^2} \sim -c^2\frac{d^2y}{dx^2}\Big/g\frac{dy}{dx} \sim \frac{c^2\alpha}{gh} \tag{6.4}$$

from equation (6.1), since for large x we have $y \sim Ae^{-\alpha x}$. From Stokes's relation

$$\frac{\tan\alpha}{\alpha} = F^2$$

it follows that $$\theta = \alpha = 1{\cdot}0495^c = 60{\cdot}13°.$$

It may be remarked that if the conjecture of Lenau (1966) that $F^2 = 3\frac{1}{2}\pi^{-1} = 1{\cdot}6540$ is correct, then $\theta = 60°$ exactly; but this conjecture is disputed by Witting (1975). For data relating to this question see Longuet-Higgins & Fenton (1974).

Figure 7 shows the trajectories that would occur in a succession of widely separated solitary waves, assuming there is no backwards flow to compensate for the forwards displacement of mass M in each wave. If owing to the presence of a beach or other obstacle the net forwards displacement is zero, then between each wave there must

X/h	Y/h	$t(g/h)^{\frac{1}{2}}$	X/h	Y/h	$t(g/h)^{\frac{1}{2}}$
0	0·830	0	2·012	0·147	3·134
0·413	0·815	0·340	2·053	0·093	3·535
0·775	0·773	0·680	2·080	0·056	3·963
1·088	0·705	1·019	2·095	0·031	4·422
1·351	0·616	1·359	2·105	0·017	4·914
1·565	0·514	1·700	2·110	0·008	5·442
1·732	0·408	2·044	2·112	0·004	6·007
1·858	0·307	2·394	2·114	0·002	6·609
1·949	0·219	2·755	2·115	0	∞

TABLE 3. Co-ordinates of points on the trajectory of a solitary wave of maximum height.

be a mean backwards displacement $-M/h$. For illustration let us suppose that the backward flow is irrotational and so uniform with depth. Hence the backwards displacement at the surface is just $-M/h$ also. In figure 8 we show the corresponding trajectories, when for M we take the value $1{\cdot}963h^2$ corresponding to the present approximation [Longuet-Higgins 1974, equation (6.14)]. In the limiting case when the separation between successive waves is infinite, then the trajectories have a sharp corner at their lowest points, but otherwise the corners will be slightly rounded. In the limiting case the net forwards displacement during one complete wave cycle is $2{\cdot}266h$. The ratio of the net horizontal displacement $[X]$ to the total height $[Y]$ of the trajectory is thus $2{\cdot}266 \div 0{\cdot}829$, or 2·73 approximately, compared with 2·67 for a wave of maximum height in deep water. It is possible that this ratio is nearly independent of the ratio of wavelength to mean water depth.

7. Subsurface particles

In § 2 we saw indications that in waves of maximum height there may be a very sharp gradient of the drift velocity for particles close to the surface. To determine the trajectories for subsurface particles in a periodic, irrotational wave in deep water we make use of the simple but very close approximation to the motion given by Longuet-Higgins (1973) in which the surface profile of six successive waves is transformed into the sides of a hexagon by the substitution

$$z = x + iy = i \ln (\zeta/\zeta_0). \tag{7.1}$$

The vertices of the hexagon correspond to six successive wave crests. When $\zeta_0 = e^{i\pi/6}$ then one vertex is on the real axis of ζ, and the trough $z = 0$ corresponds to the midpoint of one side. The wave profile is given simply by

$$y = \ln \sec x, \quad -\tfrac{1}{6}\pi < x < \tfrac{1}{6}\pi, \tag{7.2}$$

the wavelength L being normalized to $\frac{1}{3}\pi$. In the general case (7.2) becomes

$$\frac{y}{L} = \frac{3}{\pi} \ln \sec \left(\frac{\pi x}{3L}\right). \tag{7.3}$$

The crest-to-trough height is then

$$\frac{3L}{\pi} \ln \left(\frac{2}{3^{\frac{1}{2}}}\right) = 0{\cdot}1374L, \tag{7.4}$$

which differs from the accurate value $0{\cdot}1412L$ by only $0{\cdot}0038L$.

One clear advantage of this approximation is that the velocity potential χ in the interior is given by the closed expression

$$\chi = -ic \ln W, \quad |W| < 1 \tag{7.5}$$

where

$$\zeta = K \int_0^W \frac{dW}{(1-W^6)^{\frac{1}{3}}} \tag{7.6}$$

and κ is a constant:

$$\frac{2}{3^{\frac{1}{2}}K} = \int_0^1 \frac{d\rho}{(1-\rho^6)^{\frac{1}{3}}} = 1{\cdot}1129. \tag{7.7}$$

The streamlines (in the steady flow relative to axes moving with speed c) are circles in the W-plane. In fact if we write $W = \rho \exp[i(\alpha + \frac{1}{6}\pi)]$ then from (7.5)

$$\phi = c(\alpha + \tfrac{1}{6}\pi), \quad \psi = -c \ln \rho. \tag{7.8}$$

The free surface corresponds to $\rho = 1$, and the flow in the neighbourhood of a crest, say $W = 1$, is a Stokes corner-flow as it should be. Elsewhere on the free surface the pressure is very nearly constant (see Longuet-Higgins 1973, § 4).

To obtain the particle trajectories we apply the formula (3.3). Now from (7.1), (7.5) and (7.6) we have

$$\frac{dz}{d\chi} = \frac{dz}{d\zeta}\frac{d\zeta}{dW}\frac{dW}{d\chi} = \frac{i}{\zeta}\frac{K}{(1-W^6)^{\frac{1}{3}}}\frac{iW}{c}. \tag{7.9}$$

On substitution in (3.3) we obtain

$$ct = \int \left| \frac{KW}{\zeta(1-W^6)^{\frac{1}{3}}} \right|^2 d\alpha \tag{7.10}$$

and then the co-ordinates (X, Y) of the particle trajectories are given explicitly by

$$\frac{X+iY}{L} = \frac{3}{\pi}\left(i \ln \zeta + ct + \frac{\pi}{6}\right). \tag{7.11}$$

Because in this expression ct is given by (7.10) it is clear that $(X+iY)/L$ and hence U/c are formally independent of the phase-velocity c. The latter is determined from the constant pressure condition at the free surface. On the other hand, the solution (7.11) is essentially a kinematic expression determined by the free surface (7.2).

In evaluating ζ it is convenient to take the integration first along the real axis of W to the point $W = \rho$, and then along a streamline $\rho =$ constant. Thus

$$\begin{aligned} \zeta/K &= \int_0^\rho \frac{d\rho}{(1-\rho^6)^{\frac{1}{3}}} + i\int_0^\alpha \frac{\rho e^{i\alpha} d\alpha}{(1-\rho^6 e^{6i\alpha})^{\frac{1}{3}}} \\ &= F(\rho) + iG(\rho, \alpha) \end{aligned} \tag{7.12}$$

say. When $\rho = 1$, then we have in particular

$$G(1, \alpha) = e^{\frac{1}{6}i\pi} \int_0^\alpha \frac{d\alpha}{(2 \sin 3\alpha)^{\frac{1}{3}}} \tag{7.13}$$

and writing $\sin 3\alpha = s^3$ we find

$$G(1, \alpha) = \frac{e^{\frac{1}{6}i\pi}}{2^{\frac{1}{3}}}\left(\tfrac{1}{2}s^2 + \tfrac{1}{16}s^8 + \tfrac{3}{112}s^{14} + \tfrac{1}{64}s^{20} + \ldots\right) \tag{7.14}$$

which converges very rapidly when $s < 0{\cdot}5$, say. Likewise we find from (7.10)

$$ct = A + B(s - \tfrac{1}{20}Bs^5 + \tfrac{1}{14}s^7 - \ldots), \tag{7.15}$$

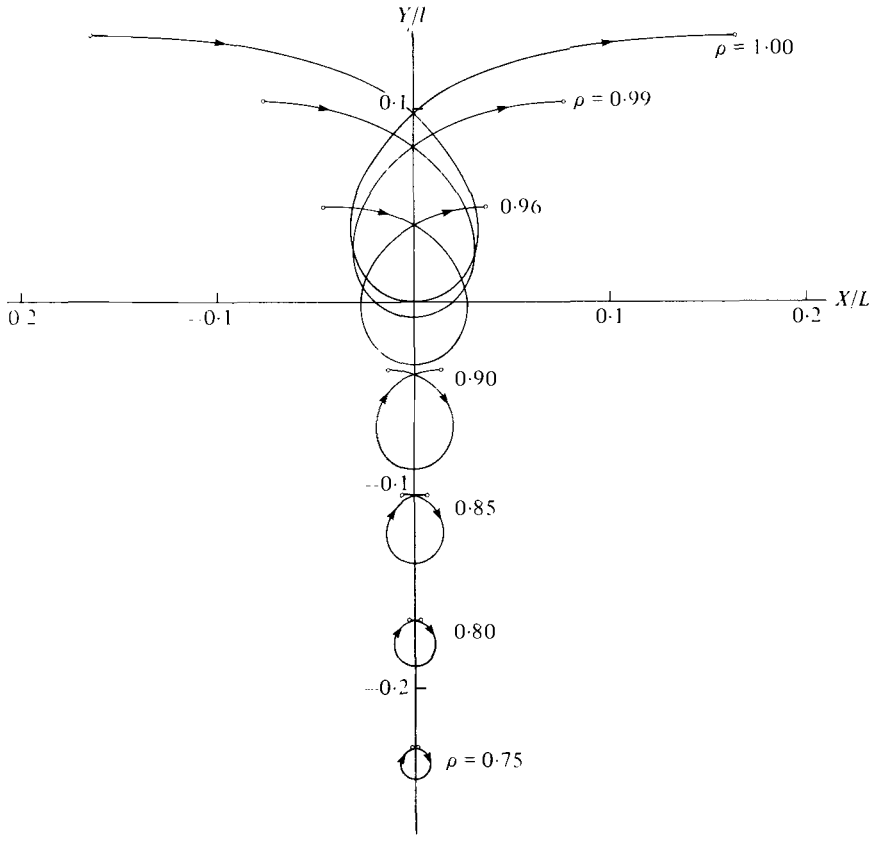

FIGURE 9. Orbits of subsurface particles in the deep-water wave of maximum steepness.

ρ	$F(\rho)$	X_{min}/L	Y_{min}/L	Y_{max}/L	$\bar{Y}/L$	$T/T_{-\infty}$	U/c
1·0	1·1129	0·1647	0	0·1374	0·0449	1·3292	0·2477
0·999	1·1047	·1261	− ·0008	·1302	·0437	·2522	·2014
0·998	1·0998	·1139	− ·0016	·1260	·0425	·2278	·1856
0·997	1·0957	·1057	− 0024	·1225	·0413	·2114	·1745
0·995	1·0887	·0942	− ·0040	·1164	·0390	·1883	·1585
0·990	1·0745	·0764	− ·0079	·1038	·0334	·1528	·1326
0·98	1·0517	·0568	− ·0160	·0833	·0224	·1136	·1020
0·97	1·0324	·0449	− ·0242	·0657	·0116	·0899	·0815
0·95	0·9990	·0303	− ·0412	·0342	− ·0097	·0607	·0572
0·90	0·9290	·0133	− ·0862	− ·0315	− ·0634	·0266	·0259
0·85	0·9163	·0062	− ·1353	− ·1001	− ·1190	·0124	·0123
0·80	0·9039	·0029	− ·1889	− ·1647	− ·1774	·0058	·0058
0·75	0·7568	·0013	− ·2472	− ·2309	− ·2393	·0026	·0026
0·70	0·7041	·0006	− ·3106	− ·2998	− ·3053	·0011	·0011

TABLE 4. Parameters of the particle orbits in a deep-water wave of maximum height: hexagon approximation.

where A is an arbitrary constant (determined by the origin of t) and

$$B = \{2^{\frac{1}{2}}F(1)\}^{-2}, \tag{7.16}$$

where $F(1)$ is the constant on the right of equation (7.7). For checking the calculations we may use the relations

$$\left.\begin{aligned}\int_0^1 \frac{d\rho}{(1+\rho^6)^{\frac{1}{3}}} &= \frac{3^{\frac{1}{2}}}{2}F(1) = \frac{1}{K},\\ \int_0^{\frac{1}{3}\pi} \frac{d\alpha}{(2\sin 3\alpha)^{\frac{1}{3}}} &= \tfrac{1}{2}F(1) = \frac{3^{-\frac{1}{2}}}{K},\end{aligned}\right\} \tag{7.17}$$

which can be derived by integration round the closed contours

$$W = (0, 1, e^{\frac{1}{3}i\pi}, 0) \quad \text{and} \quad (0, 1, e^{\frac{1}{3}i\pi}, 0).$$

In figure 9 the trajectories have been plotted for various values of ρ including $\rho = 1$ corresponding to a particle at the free surface. Other parameters, including the mean depth $\bar{y}$ of each streamline ρ constant (in the steady frame of reference), are given in table 4.

From figure 9 it can be seen how rapidly the orbital motion diminishes with the mean depth of the trajectory below the free surface. This is as we should expect from the corner-flow expression (2.20), which is of the form

$$(X+iY)/l = (h/l)P(\mu) + (h/l)^{\frac{1}{2}}Q(\mu). \tag{7.18}$$

To find U/c we must divide by the total time t taken for one complete orbit. From (2.16) this is of the form

$$ct \sim (h/l)^{\frac{1}{2}}Q(\mu). \tag{7.19}$$

Hence for large μ, U/c will behave like $(h/l)^{\frac{1}{2}}$, plus a constant, and $\partial U/\partial h$ will behave as $(h/l)^{-\frac{1}{2}}$. In figure 10(a) we have plotted U/c for the periodic deep-water wave, as a function of $(1-\rho)^{\frac{1}{2}}$. The computations confirm that U/c behaves linearly with $(1-\rho)^{\frac{1}{2}}$ near $\rho = 1$. In figure 10(b) U/c is plotted against the mean depth $\bar{y}$ of each streamline, showing that the gradient of the mean drift velocity is theoretically infinite at the free surface, where $\bar{y} = \bar{y}_0$. It is remarkable that a decrease in $\bar{y}$ of only $0{\cdot}01L$ reduces U/c to less than half its value at the free surface.

At the surface itself we have $U/c = 0{\cdot}248$, as compared to the accurate value $0{\cdot}274$ found in § 5.

These surface values may be compared with Stokes's second-order expression

$$U \doteqdot (ak)^2 c e^{2ky} \qquad (k = 2\pi/L) \tag{7.20}$$

in which it is natural to take $2a = 0{\cdot}141L$, the theoretical height of the highest wave. Thus $ak = 0{\cdot}443$ and when $y = 0$ then $U/c \doteqdot 0{\cdot}196$.

At deeper levels, however, this application of the Stokes formula leads to an overestimate of the drift velocity by a factor greater than 2. Since the exponential form of the drift velocity becomes asymptotically correct as $ky \to -\infty$, for all wave amplitudes, it is preferable to adjust the value of ak in (7.20) so as to agree with the asymptotic value as $ky \to -\infty$. By expanding ζ and ct in powers of ρ when ρ is small it may easily be shown that

$$\bar{y} \sim \ln(K\rho), \quad cT \sim \tfrac{1}{3}\pi(1+\tfrac{4}{49}\rho^{12}), \tag{7.21}$$

and so, since $k = 6$,

$$U/c = 1 - cT_\infty/cT \sim \tfrac{4}{49}\rho^{12} \sim \tfrac{4}{49}e^{2k(\bar{y}-\bar{y}_0)}, \tag{7.22}$$

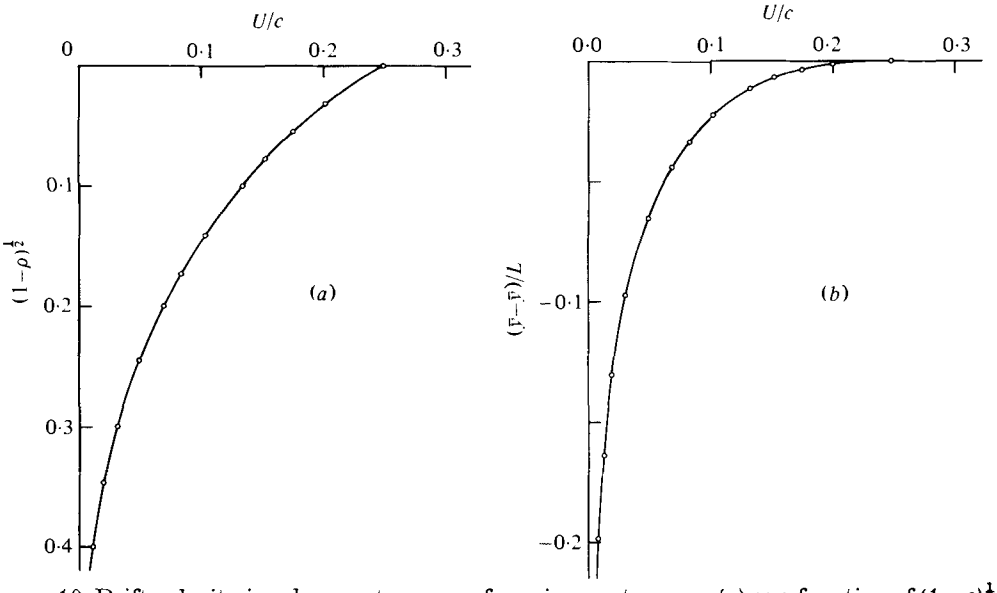

FIGURE 10. Drift velocity in a deep-water wave of maximum steepness (*a*) as a function of $(1-\rho)^{\frac{1}{2}}$, (*b*) as a function of the mean depth $\bar{y}$ of the streamline ρ = constant.

where $\bar{y}$ is the mean depth of the streamline; from which it follows that at the free surface $\bar{y} = \bar{y}_0$ Stokes's formula will give

$$U/c \doteqdot \tfrac{4}{49} = 0{\cdot}082,$$

only about one-third of the accurate value.

We may conclude that, for very steep waves, Stokes's second-order formula is not applicable over the whole range of depths.

8. Discussion

The salient feature of the drift velocity profile for a steep, irrotational wave is clearly the very strong forwards drift at the surface, with strong vertical gradient of velocity. This was to be expected from the fact that in a Gerstner wave, where (by superposing a shear) the particles are made to have *zero* drift velocity (Lamb 1932, § 251), it is found that the vorticity of the fluid has to become negatively infinite at the free surface.

It is, of course, paradoxical that in the irrotational waves that we have studied in this paper, there should be an apparent gradient in the Lagrangian mean velocity. But this effect was already well known in principle from Stokes's classic paper (1847). It may be regarded as a consequence of the fact that the integrand in the expression (3.3) for the time t is not in general an analytic function of z or of χ.

The source of the strong drift gradient has been shown in §§ 2 and 7 to be in the corner flow near to the wave crest, where the Eulerian velocity gradient becomes infinite like $r^{-\frac{1}{2}}$. When the waves are not quite at their maximum height as in § 4, this singularity disappears. On the other hand, once a whitecap has formed, it is clear that there must be a very strong vortex sheet (or shear layer) on the forwards

face of the wave. If the steady wave of maximum amplitude be regarded as a critical case separating steady breaking waves (or spilling breakers) from steady, symmetric non-breaking waves, then we see that in the strong forwards drift velocity at the surface we have, as it were, a whitecap waiting to be born.

There are at least two ways in which the present theoretical flows differ from real water waves, especially sea waves. The first is in the neglect of viscosity. We know that the condition of zero tangential stress at the free surface implies that the normal gradient of the *Lagrangian* velocity be zero (see Longuet-Higgins 1960). So we may expect that in real fluids the infinite drift-gradient at the surface will be modified by a viscous boundary layer of finite thickness $\sim (\nu/\sigma)^{\frac{1}{2}}$, where ν is the kinematic viscosity and σ is the radian frequency of the waves. Beyond this thin layer the mean drift velocity may, paradoxically, be increased by the viscosity; for waves of low amplitude, the drift gradient is known to be doubled (Longuet-Higgins 1960). As the time t after starting the motion is increased, we may expect an outer layer to grow, with thickness proportional to $(\nu t)^{\frac{1}{2}}$. Turbulence will modify the drift profile more drastically.

A second difference between ocean waves and waves in a laboratory channel is the random nature of ocean waves, the wave heights, as is well known, being distributed approximately according to a Rayleigh distribution, when the frequency spectrum is sufficiently narrow. This means that the waves are not of uniform height, either in space or time; the height of each individual wave rises to a maximum on passing through a wave group, and then diminishes (Donelan, Longuet-Higgins & Turner 1974). Thus the sharp crests or whitecaps are formed only sporadically, and at a rate of occurrence depending on the mean rate of supply of energy by the wind. Hence in practice one must expect that even in high seas, and with the assistance of whitecapping, the large drift velocities associated with steady waves of limiting height will not be attained on the average. Nevertheless, it is reasonable to suggest that some part of the 'surface wind-drift' observed in the wind-generated waves (Wu 1968) may be simply a kinematic effect associated with the irrotational motion in sharp wave crests, whenever these occur.

The action of the wind, if in the same direction as the waves, will presumably be to increase the surface shear, and thus to counteract the effects of the viscous shear stresses in the water, particularly near the wave crests. Laboratory studies of wind-generated waves (Wu 1968) indicate that the 'wind drift' velocity is about $0{\cdot}04V$, where V is the mean wind-speed in the flume. Since at these short fetches the wind-speed exceeded the phase-speed by a factor of order 15 (see Wu 1968, figure 4) this indicates ratios U/c of the order of 0·6, certainly greater than the kinematic effect alone would account for. Moreover the drift velocity profiles are nearly linear with depth, indicating the predominant role played by turbulent mixing, under these conditions.

The most directly relevant application of our results is, therefore, likely to be in the interpretation of drift velocity measurements in channels with mechanically generated waves, such as reported briefly by Nath (1978). Here the velocities of buoys, spheres and floating discs were measured in a flume 104 m long, 3·7 m wide and 3·4 m deep, in the presence of regular waves with periods ranging from 1 to 4 s. The experiments were made under conditions where the influence of wind on the surface currents might be expected to be slight. The maximum values of U/c that

were observed were those for the small discus, whose speed generally exceeded that of the small sphere by a factor of between 1·2 and 1·5. This indicates a drift gradient within a distance from the surface of the same order as the diameter (3·7 cm) of the sphere. On the other hand the observations appear not to have been made in waves of less than maximum height and then extrapolated *linearly* up to the assumed limit. The maximum values of U/c so estimated were about 0·15. This value is consistent with the finding in § 2 of this paper that only a very small departure of the waves from their steady, limiting conditions will sharply reduce the surface drift velocity.

In addition it must be pointed out that the theoretical values of U/c will be quite sensitive to small changes in the phase-velocity due, for example, to a finite depth of water or, in laboratory channels, to a net backward flow compensating the forwards mass transport. Thus a change in c of only 15 per cent would be enough to reduce the theoretical value of U/c from 0·27 for waves in infinitely deep water to 0·16, about the same as reported by Nath. Further experiments are desirable in order to determine which of the effects just mentioned was dominant.

In this paper, we have not attempted an investigation of the stability of the flows under consideration. Nevertheless in regions of strong velocity gradient, such as occur near the wave crest, it is to be expected that viscous stresses will tend to destabilize the flow, quite apart from the non-viscous modes of instability already known (Longuet-Higgins 1978*a*, *b*) which have been shown to lead swiftly to overturning of the free surface (Longuet-Higgins & Cokelet 1979). If viscous instabilities having comparable rates of growth can be shown to exist, then another mode of wave breaking will have been established.

REFERENCES

Bowman, F. 1953 *Elliptic Functions*. New York: Wiley.

Cokelet, E. D. 1977 Steep gravity waves in water of arbitrary uniform depth. *Phil. Trans. Roy. Soc.* A **286**, 183–260.

Donelan, M., Longuet-Higgins, M. S. & Turner, J. S. 1972 Periodicity in whitecaps. *Nature* **239**, 449–451.

Jahnke, E., Emde, F. & Losch, F. 1960 *Tables of Higher Functions*, 6th ed. New York: McGraw-Hill.

Lamb, H. 1932 *Hydrodynamics*, 6th ed. Cambridge University Press.

Lenau, C. W. 1966 The solitary wave of maximum amplitude. *J. Fluid Mech.* **26**, 309–320.

Longuet-Higgins, M. S. 1960 Mass transport in the boundary layer at a free oscillating surface. *J. Fluid Mech.* **8**, 293–306.

Longuet-Higgins, M. S. 1963 The generation of capillary waves by steep gravity waves. *J. Fluid Mech.* **16**, 138–159.

Longuet-Higgins, M. S. 1973 On the form of the highest progressive and standing waves in deep water. *Proc. Roy. Soc.* A **331**, 445–456.

Longuet-Higgins, M. S. 1974 On the mass, momentum, energy and circulation of a solitary wave. *Proc. Roy. Soc.* A **337**, 1–13.

Longuet-Higgins, M. S. 1978*a* The instabilities of gravity waves of finite amplitude in deep water. I. Superharmonics. *Proc. Roy. Soc.* A **360**, 471–488.

Longuet-Higgins, M. S. 1978*b* The instabilities of gravity waves of finite amplitude in deep water. II. Subharmonics. *Proc. Roy. Soc.* A **360**, 489–505.

Longuet-Higgins, M. S. 1979 The almost-highest wave: a simple approximation. *J. Fluid Mech.* **94**, 269–274.

LONGUET-HIGGINS, M. S. & COKELET, E. D. 1978 The deformation of steep surface waves on water, II. Growth of normal-mode instabilities. *Proc. Roy. Soc.* A **354**, 1–28.

LONGUET-HIGGINS, M. S. & FENTON, J. D. 1974 On the mass, momentum, energy and circulation of a solitary wave. II. *Proc. Roy. Soc.* A **340**, 471–493.

LONGUET-HIGGINS, M. S. & FOX, M. J. H. 1977 Theory of the almost-highest wave: the inner solution. *J. Fluid Mech.* **80**, 721–741.

LONGUET-HIGGINS, M. S. & FOX, M. J. H. 1978 Theory of the almost-highest wave. Part 2. Matching and analytic extension. *J. Fluid Mech.* **85**, 769–786.

NATH, J. H. 1978 Drift speed of buoys in waves. *No.* 6, *Summaries of Papers*, 16*th Inst. Conf. on Coastal Engng, Hamburg, August* 27–*September* 3.

RAMSEY, A. S. 1937 *Dynamics*, Part II. Cambridge University Press.

RAYLEIGH, LORD 1876 On waves. *Phil. Mag.* (5) **1**, 257–279.

SCHWARTZ, L. W. 1974 Computer extension and analytic continuation of Stokes' expansion for gravity waves. *J. Fluid. Mech.* **62**, 553–578.

STOKES, G. G. 1847 On the theory of oscillatory waves. *Trans. Cam. Philos. Soc.* **8**, 441–455.

STOKES, G. G. 1800 On the theory of oscillatory waves. Appendix B. *Math. and Phys. Pap.* **1**, 225–228.

VON SCHWIND, J. S. & REID, R. O. 1972 Characteristics of gravity waves of permanent form. *J. Geophys. Res.* **77**, 420–433.

WITTING, J. 1975 On the highest and other solitary waves. *SIAM J. Appl. Math.* **28**, 700–719.

WU, J. 1968 Laboratory studies of wind-wave interactions. *J. Fluid Mech.* **34**, 91–111.

YAMADA, H. 1957 Highest waves of permanent type on the surface of deep water. *Rep. Res. Inst. Appl. Mech. Kyushu Univ.* **5**, 37–57.

YAMADA, H. 1958 On approximate expressions of solitary waves. *Rep. Res. Inst. Appl. Mech. Kyushu Univ.* **6**, 35–47.